

# Quantitative Analysis of Carcinoembryonic Antigen (CEA) Using Micromechanical Piezoresistive Cantilever

Meisam Omid, M. Mirijalili, Mohammadmehdi Choolaei, Z. Sharifi, F. Haghirsadat, F. Yazdian

**Abstract**—In this work, we have used arrays of micromechanical piezoresistive cantilever with different geometries to detect carcinoembryonic antigen (CEA), which is known as an important biomarker associated with various cancers such as colorectal, lung, breast, pancreatic, and bladder cancer. The sensing principle is based on the surface stress changes induced by antigen–antibody interaction on the microcantilevers surfaces. Different concentrations of CEA in a human serum albumin (HSA) solution were detected as a function of deflection of the beams. According to the experiments, it was revealed that microcantilevers have surface stress sensitivities in the order of 8 (mJ/m). This matter allows them to detect CEA concentrations as low as 3 ng/mL or 18 pM. This indicates the fact that the self-sensing microcantilevers approach is beneficial for pathological tests.

**Keywords**—Micromechanical biosensors, Carcinoembryonic antigen (CEA), surface stress.

## I. INTRODUCTION

**M**ICRO-ELECTROMECHANICAL SYSTEMS (MEMS) have been extensively investigated as biosensor platforms due to their ability to generate highly sensitive and quantitative measurements without the cost, complexity, or labeling. Among all different MEMS sensors, Micromachined silicon cantilevers are considered as the simplest type, which have the ability be micromachined and mass-produced. Microcantilever sensor technology allows us to detect extremely small forces, mechanical stresses, and mass additions with a considerable sensitivity. According to these stunning potentials, Micro-cantilever technology illustrates broad applications in chemical, physical, and biological detection [1]-[4].

It is possible to operate Micro-cantilever sensors in two different modes, static mode (surface stress method) and dynamic mode (microbalance method). In the static mode, the induced surface stress that is due to the presence of the adsorbates results in a deflection in the cantilever [5], while in the second mode, dynamic mode, the adsorbates change the resonance frequency of a cantilever due to mass loading. The

most important demerit of the dynamic detection mode could be the cantilever damping in a liquid environment resulting in a change in the quality factor (Q-factor). Moreover, a change in the medium viscosity could lead to an undesirable resonant frequency change [6]. In cases where viscous damping reduces the sensitivity to detect shifts in resonance frequency, such as liquid-based bio-sensing, the adsorption-induced cantilever bending (static mode) could be an ideal method for detection.

A sensitive readout system is crucial for monitoring the deflection of cantilevers. For that reason several read-out methods have been presented. Among the most extended readout methods for biosensing are optical, and piezoresistive ones. The optical method is simple to implement and shows a linear response with sub-angstrom resolution, also is currently the most sensitive method. This method is employed for detecting the cantilever deflection in most studies [6]-[9]. Nevertheless, the optical detection mechanism present some disadvantages for example, bulky, time-consuming laser alignment on each cantilever, low applicability for large one- or two-dimensional arrays, and the difficulty of performing measurements in opaque liquids, such as blood that may hinder the potential application of this method for actual applications. The piezoresistive sensing method is known as good alternative for the optical detection in biosensing application. The benefits of this method are that the principle works well in both liquid and gas phase and large arrays can be realized and read-out. Also, the technique is applicable for static as well as dynamic measurements [10]-[13].

Cancer diagnosis and treatment are of great interest because of the widespread occurrence of the diseases, high death rate, and recurrence after treatment. According to the National Cancer Institute, Lung cancer, breast cancer and prostate cancer are considered as the most prevalent form of cancer in Unite State. Carcinoembryonic antigen (CEA) is a glycoprotein involved in cell adhesion. It is normally produced in gastrointestinal tissue during fetal development, but the production of CEA stops before birth. Therefore, it is usually present only at very low levels in the blood of healthy adults, although levels are raised in heavy smokers [14], [15]. Research findings indicate the importance of CEA as a useful marker for early detection of various cancers such as colorectal, lung, breast, pancreatic, and bladder cancer, monitoring patients for disease progression, and studying the effects of treatment [16], [17]. It is worth mentioning that the critical value of CEA concentration is known as 5 ng/ml.

In this study, the performance of the fabricated

M. Omid, F. Haghirsadat, and F. Yazdian are with the Faculty of New Science and Technology University of Tehran, Tehran, Iran (phone: 918-331-2585; e-mail: m\_omidi@ut.ac.ir).

M. Choolaei, was with Research Institute of Petroleum Industry (RIPI), Tehran, Iran.

Z. Sharifi is with the Faculty of Social Sciences and Economics, Alzahra University, Tehran, Iran.

M. Mirijalili is with the Faculty of Engineering, Islamic Azad University, Yazd Science and Research Branch.

micromechanical piezoresistive cantilever was studied by using different concentrations of CEA in human serum albumin (HSA). A direct nano-mechanical response of microcantilever was used to detect the surface stress changes of antigen-antibody specific binding. After injecting the CEA target, as model biocontents, the piezoresistive responses were carefully analyzed and the feasibility of the piezoresistive microcantilever for biosensing were discussed in terms of device performance measures such as sensitivity, accuracy, and specificity..

## II. EXPERIMENTAL REVIEW STAGE

### A. Fabrication of Microcantilever Sensor

We used Silicon on Insulator (SOI) wafers with a 2 $\mu$ m device layer and a 0.3 $\mu$ m buried oxide (BOX) layer as the substrate material. Then a 25nm silicon dioxide layer was grown by a thermal oxidation to electrically insulate the device layer from the subsequent metal layers. The first lithographic process to define the first metal layer for electrode and sensor platform for subsequent liftoff process has been accomplished. After patterning, the photoresist, chrome (10nm) and gold (50nm) layers were deposited by e-beam evaporator and patterned by a liftoff process with the previously patterned photoresist. The patterned metal layer from previous step and the patterned layer of photoresist, from the second photolithographic process were used to define the areas to be etched to define the sensor structure. The exposed device layer was etched completely by RIE to define the sensor structure. Then, a third photolithographic step for the second liftoff process, followed by the deposition of a 30-nm chrome layer and a 150-nm gold layer for wire-bonding pads. After the liftoff, a release window was photolithographically defined by the fourth lithographic process and the exposed BOX was etched by RIE leaving the Si substrate exposed. Then the wafer was diced into individual chips. Through the release window, the exposed Si substrate was etched by vapor phase etching using xenon difluoride (XeF<sub>2</sub>) to release the sensor structure. After XeF<sub>2</sub> etching, the photoresist and the BOX were removed by BHF etching and solvent cleaning. The die was cleaned with oxygen plasma and then a 100-nm thick silicon dioxide layer was deposited with plasma enhanced chemical vapor deposition (PECVD) for insulation. Chrome (20nm) and gold (50nm) layers were deposited using an e-beam evaporator for an immobilization layer for protein-protein interaction. The PECVD oxide on the bonding pads was selectively etched for wire-bonding. Then each die was attached to a custom made printed circuit board (PCB) and was wire-bonded. For the electrical measurement of sensor, internal dc-bias Wheatstone bridge was used. A bridge supply voltage of 4.5V was applied using a dc power supply (Agilent, E3631A), and the sensor output voltage was measured by a multimeter (Keithley, 2010 7-1/2), which was 100 times amplified by an instrumentation amplifier (Analog Device, AD624). Moreover, a Faraday cage was adopted for noise reduction. The above components were used to measure the piezoresistive response of the microcantilever in a liquid

environment.

Fig. 1 presents the final picture of microcantilever array chip using a Scanning electron micrograph (SEM) and schematic of the on-chip half Wheatstone bridge, where two resistors are placed on microcantilever. In the case of piezoresistors, heating of the resistors when voltage is applied is an additional concern. However, this can be compensated by a thermally symmetric design. One microcantilever was coated with a biologically active layer on its upper surface (active microcantilever), and the other was inactive (reference microcantilever). The lower surfaces of both cantilevers were inactive also biologically. The active microcantilever can be deflected by both biomolecular interactions and environmental noise such as thermal drift, while the reference microcantilever is affected only by environmental noise. Accordingly, we can obtain the true piezoresistive response of the active microcantilever due to the biomolecular interaction through compensation of the environmental noise using the reference microcantilever.

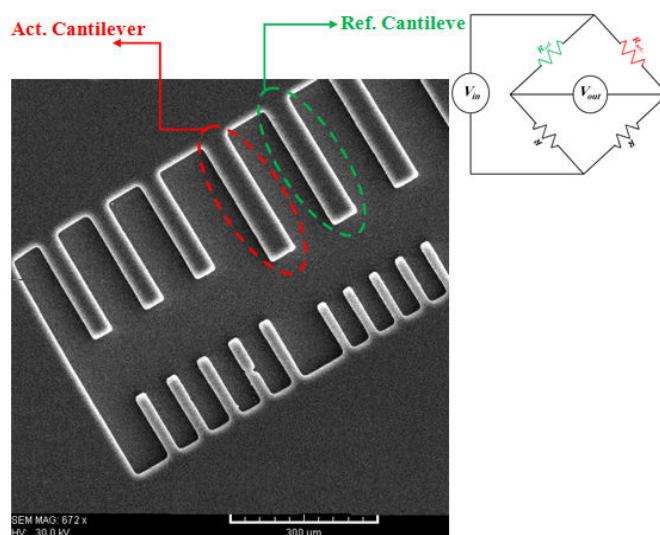


Fig. 1 Scanning electron micrograph (SEM) of the fabricated microcantilever array chip with a schematics of the on-chip Wheatstone bridge, where two resistors are placed on cantilever

### B. CEA Antibody Immobilization Process

A fresh piranha solution (a 4:1 ratio of H<sub>2</sub>SO<sub>4</sub> (98.08%) and H<sub>2</sub>O<sub>2</sub> (34.01%)) was used to wash and clean the membranes, in order to remove experimental contamination of the Au surface. After 1min, the membranes were taken out of the solution and were rinsed using deionized water. To complete the cleaning process, the rinsed membranes were dried using a stream of N<sub>2</sub> gas. For 2 h at room temperature in darkness a 0.1M deoxygenated cysteamine (Sigma, 95%) aqueous solution was used to functionalize the devices. Then, microcantilevers were washed with deionized water and soaked in water for 12h to remove the physically adsorbed cysteamine. Moreover, for creating a covalent cross-linker molecule between the amine groups on the microcantilever surface and antibodies, chips were soaked in a 5% solution of glutaraldehyde (Sigma, 50%) in borate buffer for 2 hours.

Following this and all subsequent steps, device chips were washed twice, each washing step was for two minutes, in purified DI water on an orbital shaker operating at 95 RPM. It should be mentioned that fresh water was used between washes. The reason of using water instead of buffer for washing was to prevent the abundant formation of buffer salt crystals on the surface of devices which make the sensors effectively useless.

Next, one hour incubation was used to immobilize the monoclonal anti-CEA (Anti-carcinoembryonic, Sigma), affinity-purified, with a concentration of 50mg/mL on the surface. By immersing the microcantilever in 50mM solution of glycine for 30 minutes unreacted gluteraldehyde was then quenched. In addition, dissolved bovine serum albumin (BSA, Sigma) in phosphate buffered saline (PBS) with 10mg/ml concentration was used to prevent non-specific binding. For this purpose, the membranes were immersed in this solution for 1h at room temperature. Then, they were rinsed with PBS (pH 7.4) containing polyoxyethyethylenesorbitan monolaurate (Tween 20) and finally washing was performed by only using PBS solution.

### III. RESULTS AND DISCUSSION

If In order to reach results with high reliability, the surfaces of the membranes were stabilized by treating them with a PBS buffer. The PBS buffer was directed with a typical flow rate of 0.4 – 0.5ml/hour, for 1h, to the microcantilever sensor arrays using a flexible PDMS polymer microfluidic channel sealed to the device chip. As a general trend, at the point of initial injection of the PBS buffer the induced voltage of the microcantilever increased rapidly and steadily decreased with time, which in this case the induced voltage of the microcantilever reached dynamic equilibrium after 10min. For the bio-assay, CEA antigens were injected into each liquid chamber, including the stabilized microcantilever. The liquid temperature was precisely controlled and external noise sources were excluded using a shield box. In order to estimate the nonspecific adsorption on the microcantilever surface, the concentration of HSA in all solutions was stabilized at 0.1 mg/ml.

In the surface-stress microcantilever biosensors, the change in surface free energy of one surface of the microcantilever is the main reason of cantilever deflections. The value of the cantilever deflection,  $\Delta z$ , can be estimated from Stoney's formula [18];

$$\Delta z = \frac{3(1-\nu)l^2}{Et^2} \sigma \quad (1)$$

where  $\sigma$  is the change in surface free-energy density (or surface stress) due to specific binding,  $E$  is the elastic modulus of the cantilever material,  $\nu$  is its Poisson ratio, and  $l$  and  $t$  are the length and the thickness of the microcantilever, respectively. In the piezoresistive based microcantilever, the resistance of a doped region on a cantilever changes reliably when the cantilever is stressed with deflection. The variation

in cantilever resistance can be measured using an external, Wheatstone bridge.

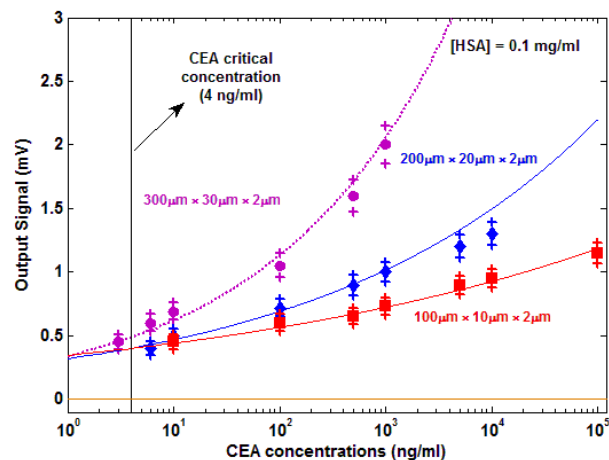


Fig. 2 Steady-state output signals ( $V_{out}$ ) as a function of CEA concentrations for three different cantilever geometries. Every data point on this plot represents an average of cantilever deflections obtained in multiple experiments done with different cantilevers, whereas the range of deflections obtained from these experiments is shown as the error bar. The error bar in each of these data points represents the fluctuation of the cantilever during the particular measurement

Fig. 2 shows the steady-state output signals ( $V_{out}$ ) as a function of CEA concentration in a HSA background for different lengths,  $l$  of cantilevers. Using 100 $\mu$ m-long and 2 $\mu$ m-thick cantilevers, the lowest CEA concentration that we could clearly detect above noise was 10ng/ml. However, when we used 300 $\mu$ m-long and 2 $\mu$ m -thick microcantilever, CEA concentration as low as 3ng/ml was detectable which is close to the critical concentration of CEA [16], [17]. The experimental results presented a range of linearity of 3ng/mL to 1 $\mu$ g/mL, 5ng/mL to 10 $\mu$ g/mL and 10ng/mL to 100 $\mu$ g/mL for 300 $\mu$ m x 30 $\mu$ m x 2 $\mu$ m, 200 $\mu$ m x 20 $\mu$ m x 2 $\mu$ m and 100 $\mu$ m x 10 $\mu$ m x 2 $\mu$ m microcantilever, respectively. The minimum detectable surface stress for each sensor can be obtain when the output signals are equal to the noise values. By using the experimental results and (1), 8mJ/m was the minimum surface stress sensitivities for microcantilevers.

### IV. CONCLUSIONS

Use In the present study, we have experimentally investigated the electrical detection of carcinoembryonic antigen using piezoresistive self-sensing microcantilevers with different geometries. From the above experiment, it was shown that antigen-antibody interaction generated compressive stress on the thin-film piezoresistive self-sensing microcantilevers. Compressive surface stress was induced throughout the microcantilevers, resulting in microcantilevers bending and resistance change of the piezoresistive layer. The sensor output voltage of the piezoresistive microcantilevers was proportional to the CEA concentration in the HSA solution. The high sensitivity of these microcantilevers arrays

makes them favorable candidates for many applications, including miniaturized sensors and multiplexed detection systems.

#### REFERENCES

- [1] N. V. Lavrik, M. J. Sepaniak and P. G. Datskos, *Rev. Sci. Instrum.*, 2004, 75(7), 2229.
- [2] Arlett J.L., Myers E.B. and Roukes M.L., *Nat. Nanotechnol.*, 2011, 6, 203.
- [3] Boisen A., Dohn S., Keller S. S., Schmid S. and Tenje M., *Rep. Prog. Phys.*, 2011, 74, 036101.
- [4] Alvarez M. and Lechuga L. M., *Analyst*, 2010, 135, 827.
- [5] Wu G., Datar R.H., Hansen K.M., Thundat T., Cote R.J. and Majumdar A., *Nat. Biotechnol.*, 2001, 19, 856.
- [6] Omid M., Malakoutian M. A., Choolaei M., *Chin. Phys. Lett.*, 2013, 30(6), 068701.
- [7] Thundat T., Warmack R. J., Chen G. Y. and Allison D. P., *Appl. Phys. Lett.*, 1994, 64, 2894.
- [8] Lang H. P., Baller M. K., Berger R., Gerber C., Gimzewski J. K., Battiston F. M., Fornaro P., Ramseyer J. P., Meyer E. and Guntherodt H. J., *Anal. Chim. Acta* 1999, 393, 59.
- [9] Ghatkesar M. K., Lang H. P., Gerber C., Hegner M. and Braun T., *PLoS One*, 2008, 3, 3610.
- [10] Mukhopadhyay R., Sumbayev V. V., Lorentzen M., Kjems J., Andreasen P. A. and Besenbacher F., *Nano Lett.*, 2005, 5, 2385.
- [11] Aeschimann L., Meister A., Akiyama T., Chui B. W., Niedermann P., Heinzlmann H., De Rooij N. F., Staufer U. and Vettiger P., *Microelectron. Eng.*, 2006, 83, 1698.
- [12] Arlett, J. L.; Maloney, J. R.; Gudlewski, B.; Mulneh, M.; Roukes, M. L. *Nano Lett.*, 2006, 6, 1000.
- [13] Boisen A. and Thundat T., *Mater. Today*, 2009, 12, 32.
- [14] Perkins, S. J., *FEBS Lett.*, 2000, 475 (1), 11.
- [15] Thomas SN, Zhu F, Schnaar RL, Alves CS, Konstantopoulos K., *J Biol Chem.*, 2008, 283 (23), 15647.
- [16] Brian B., Shaker A M., *Nanotech. Sci. Applic.*, 2011, 4, 1.
- [17] Noelia D., Paula D., Sergio M., Maria G., Sara P., Alberto O. and Manuel F., *Sens.*, 2012, 12, 2284.
- [18] Stoney G. G., *Proc. R. Soc. Lond.*, 1909, A(82), 172.